



# Dry Sliding Friction and Wear Performance of HVOF Sprayed WC–Co Coatings Deposited on Aluminium Alloy

G. S. Pradeep Kumar<sup>1</sup> · R. Keshavamurthy<sup>2</sup> · V. Umesh<sup>1</sup> · Vijay Tambrallimath<sup>3</sup> · Yash Yadav<sup>1</sup> · Talha Toufeeq<sup>1</sup> · Sakshi Arun<sup>1</sup>

Received: 20 June 2021 / Accepted: 6 August 2021 / Published online: 9 September 2021  
© The Institution of Engineers (India) 2021

**Abstract** The tribological behaviour of WC–Co Cermet coatings coated on Al6061 alloy was studied in this work. WC–Co Cermet coatings have been coated with different thicknesses by changing the amount of the cobalt using HVOF (High velocity oxy fuel technique). The coatings produced have been subjected to microhardness, friction and wear testing. A disc and pin type machine has been used for assessing friction and wears characteristics. The influence on tribological performance of coating thickness and cobalt levels was examined and compared with aluminium alloy. WC–Co coating enhanced hardness by 34% and 42% in 100 and 200 micron thicknesses respectively, compared to aluminium alloy. The wear rate and the coefficient of friction are decreased by 48 and 12%, respectively, compared to uncoated aluminium alloy. Both coatings and substrates increase their wear rate and friction coefficient (COF) with the increase in load and sliding speed. Scanning Electron and Confocal microscopy examinations of worn surfaces were carried out to evaluate coating wear processes.

**Keywords** HVOF coatings · WC–Co · Al6061 alloy · Friction and wear · Hardness

## Introduction

For many technical applications, aluminium alloys offer a high strength-to-density relation. Aluminium alloys have low tribological characteristics and corrosion resistance despite this favourable trait, resulting in increased wear in hostile environmental circumstances [1, 2]. In recent years, several surface modification techniques have been effectively utilised to improve the aluminium alloy surface characteristics. Thermal spray coating techniques are among the numerous accessible surface coating processes, especially for wear and corrosion resistant coating development. Because a variety of technical materials including ceramics and metals may be deposited, thermal spray methods provide a number of benefits over alternative surface deposition processes [3].

The technique of coating with HVOF (High Velocity Oxy Fuel) is commonly used for applying coatings on surfaces heated to or with greater melting points. A gas jet, created with the use of oxygen and the fuel in a combustion chamber, is mixed and burnt at high pressure and temperature and powdered onto the surface of the substrate before it is injected into it. Coats are deposited at greater velocity and lower temperatures compared to conventional thermal coating techniques. This allows a denser covering with less porosity and less oxide formation. The HVOF technique may create high density and hardness coatings, as well as outstanding bonding strength and toughness [4–10]. In severe conditions of the environment, when wear and corrosive resistance are important, WC-based cermet coatings for engineering components are generally preferred [11]. When WC coatings are produced using the HVOF technique, they usually have very good resistance to wear, adhesion strength, hardness and low porosity.

---

✉ R. Keshavamurthy  
keshavamurthy.r@gmail.com

<sup>1</sup> Department of Mechanical and Automobile Engineering, CHRIST (Deemed to be University), Bangalore, India

<sup>2</sup> Department of Mechanical Engineering, Dayananda Sagar College of Engineering, Bangalore, India

<sup>3</sup> Department of Automobile Engineering, Dayananda Sagar College of Engineering, Bangalore, India

Cermets form an excellent coating structure, coated in a mix of softer metal matrix (CoCr, Co, Ni, NiCr, etc.) and hard particles (WC). The WC phase offers wear resistance and hardness in this structure, while the metal matrix gives the necessary toughness. Due to unmelted WC particles and the deposited metal binder on a substrate, the structure of the coating is lamellae. Reactions between metal matrix and carbide can produce phase changes in coatings depending on the spraying circumstances and temperatures. Primary reactions include mixed decomposition of  $W_xCo_yC_z$  and/or tungsten metal, and breakdown of WC to  $W_2C$ . This decomposition can have an influence in particular on the wear characteristics of coatings. WC-based coats are one of the most durable coatings available, which can survive sliding, or erosion, corrosion and abrasion in various circumstances.

A lamellar grain structure produced by HVOF causes the fast solidification partially on tiny particles, flattened by high velocity on a cold surface. During the thermal spray process, tungsten carbide oxidation decarburization leads to the production of both  $W_2C$  and W in the coating [12]. As the binder phase approaches the melting point, solubility processes begin to dissolve the toilet crystals, resulting in an increased quantity of carbon and tungsten during the binding phase [13]. HVOF can provide low oxidation, low carbide breakdown and low porosity coatings. A smaller size of carbide grain is a major parameter for the mechanical characteristics and the wear behaviour of carbide coatings which have an advantage in wear performance [14]. Deposition of good quality coatings is increasingly challenging when the size of grain decreases owing to tiny particles which are prone to overheating and can lead to oxidation and decarburisation [15]. Fine grain size feedstock and optimum process conditions are necessary to obtain acceptable coatings [16]. The wear and friction characteristics of ceramic coatings placed on steel components were studied under dry sliding circumstances by Pirso et al. Three different cermets were tested on steel discs, consisting of chromium carbides, titanium and tungsten. On a modified block-on-ring machine, sliding wear tests were performed. The wear strength and friction coefficient are demonstrated to be modified by metal type and composition. In WC–Co cermets, wear resistance was determined to be the greatest. The wear rate of the cermets TiC–NiMo and WC–Co rises as the cermets' binder concentration increases. The wear of  $Cr_3C_2$ –Ni cermets is considerably harder and depends on the composition of the cermet [17]. Yuan et al. [18] investigated the effect on the sliding wear behaviour of the WC–Co coatings by introducing submicron-size WC particles. To mix commercial WC–12Co powder, ball friction was employed. The microhardness of the coatings has been improved to over 1400 HV by 5%, up from approximately 1150 HV with the conventional WC–12Co cover. Sliding tests with  $Si_3N_4$

balls as counterparts were conducted at room temperature. The submicron particles in the splat surfaces prevented the spread of wear fractures, which resulted in decreased wear rate. Terajima et al. have tried to employ WC–12Co as a foundation for improving the wear resistance of amorphous Fe-based coatings (FeCrMoCB). The WC–Co reinforcement particles had been tested at 2%, 4% and 8% of the weight. Without using WC–Co particles, the coating was evaluated. The porosity of the Fe-based layer was higher than that of the WC–Co particle strengthened layer. Carbides, used on splat interfaces to fill the holes, were found. With the increase in WC–Co percentage, the microhardness increased from 700 to 900 HV. To study the sliding behaviour of the coatings, a reciprocal tribometer with an alumina ball was employed. The friction coefficient decreased from 0.8 to about 0.6 on increasing the amount of WC–Co particles [19]. Utu et al. [20] have utilised high-speed oxygen fuel (HVOF) spray to produce coatings WC/20CrC<sub>7</sub>Ni and WC/10Co4Cr on low-carbon steel substrates. The microstructure of the coatings produced was examined using scanning electron microscopy (SEM). In order to assess the wear resistance of the coatings, the samples were abraded using rubber wheel. As far as abrasion wear is concerned, the test results showed that the WC–CrC–Ni coating exceeds WC–CoCr coating [21].

Serbban et al. focussed on the wear resistance of cermet based hard WC coatings. The technology of high-speed oxygen fuel (HVOF) was utilised to produce coatings on low carbon steel substrates utilising 2 WC-10.0% Co-40% Cr and WC-20% CrC-70% Ni containing powders. The resistance of sliding wear was determined by the pin-on-disc technique. The WC–CoCr coating was found to be superior to the wear-induced WC–CrC–Ni coating [22]. For the production of WC–Co and WC–CoCr coatings, Varol et al. [23] utilised the HVOF method on three different aluminium alloy substrates. Depending on the coating and substratum type, the characteristics of the coatings were studied in terms of microstructures and wear. WC–CoCr coatings have been shown to be tougher compared to WC–Co coatings. The inclusion of Cr in the coating also enhanced the binding of carbide grains. Based on these parameters, WC–CoCr coatings outperformed WC–Co coatings in terms of wear resistance on all alloy substrates.

The present work employed the HVOF method to produce the WC–Co cermet coating by changing the thickness of the cobalt.

Al6061 alloy was chosen as a substrate material. Load and sliding speed were varied to study, the influence of cobalt content on dry sliding friction and wear properties of ceramic coatings. Wear and friction tests were performed using a pin on the disc tribometer. For the investigation of wear phenomena, confocal microscopy and scanning electron microscopy were adopted.

## Materials and Methods

Given its widespread use in the industrial sector, Al6061 alloy was chosen as the material for the substrate. WC–Co powders, with variable cobalt content, were utilised as a feedstock for the HVOF deposition process. The structure and chemistry of the WC–Co coating particles are presented in Fig. 1a, b, respectively. WC–Co particles are spherical with size ranging from 40 to 60 microns. Scanned electron microscopy (SEM) and energy-dispersive spectroscopy (EDS) have been employed to verify WC–Co particle size and content (EDS). The proportion of cobalt in WC–Co powder ranged from 10 to 20 wt%, respectively.

To increase surface roughness, the alloy substrate Al6061 was sand-blasted before applying the HVOF coatings. HVOF experiments were carried out at M/s Spraymet Technologies Private Limited, Peenya, Bangalore, India. A bond coat of 30 microns of NiMoCr was placed before the deposition of WC–Co on aluminium alloy. Coating thicknesses of 100 microns and 200 microns were established on the substrata; Table 1 provides the parameters for HVOF deposition utilised in this investigation. Microstructure investigations, friction wear tests and hardness testing were undertaken on the produced WC–Co composite layers. Micrographs of metallographically polished cross sections and the top surfaces of coated coatings were acquired using scanning and optical electron microscopy. The hardness of the deposited coatings was tested in accordance with the ASTM E92 standards with 100 g load and 20 s loading duration. Five hardness tests have been recorded for each sample and five values have been averaged to determine hardness.

### Friction and Wear Tests

A disc-pin was utilised for sliding test at room temperature with a sliding speed of 0.314–1.257 m/s and a load range

**Table 1** Coating parameters

Sl. No.	Parameter	Value
1	LPG (propylene flow)	$1.5 \times 10^{-3} \text{ m}^3/\text{s}$
2	Oxygen flow	$5.5 \times 10^{-3} \text{ m}^3/\text{s}$
3	Air flow	$6 \times 10^{-3} \text{ m}^3/\text{s}$
4	Carrier gas-Nitrogen	$2.5 \times 10^{-3} \text{ m}^3/\text{s}$
5	Powder feed rate	$0.5 \times 10^{-3} \text{ kg/s}$
6	Standoff distance	1.88 m
7	Powder size	40–60 microns

of 25–100 N. (Make: Ducom, Bangalore, India). Friction and wear properties have been tested as per the ASTM-G99 method against the steel disc. For each test, the frictional coefficient was computed using frictional force and applied load data. In order to calculate the wear rate of the coating, wear in the form of height loss were measured. Before the wear test, surfaces of these specimens were polished and surface roughness was evaluated to guarantee a single micron finish. For all experiments, the wear track diameter has been set to 40 mm to increase data reliability; each test has been duplicated twice on fresh samples. After the wear test the worn-out surfaces were checked for the mechanisms of material loss with scanning electron microscopy and confocal microscopy.

## Results and Discussion

### Characterisation deposited coatings

Figures 2 and 3 depict optical and SEM representations of both cross sections. Both coatings have densely packed lamellae structures and show no signs of cracking. As there is no delamination at the interface, good adhesion with the

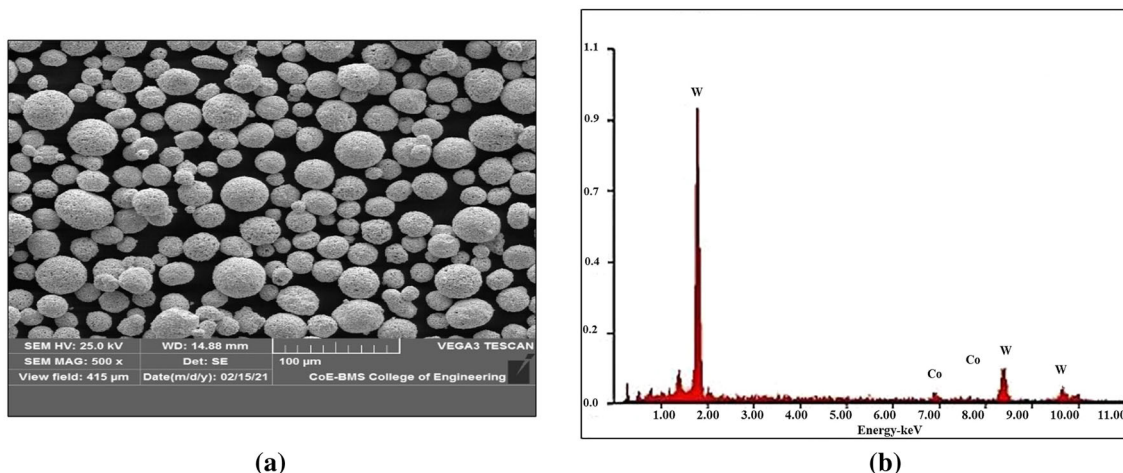
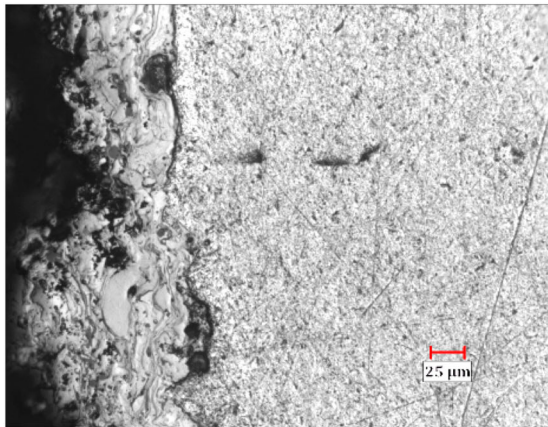
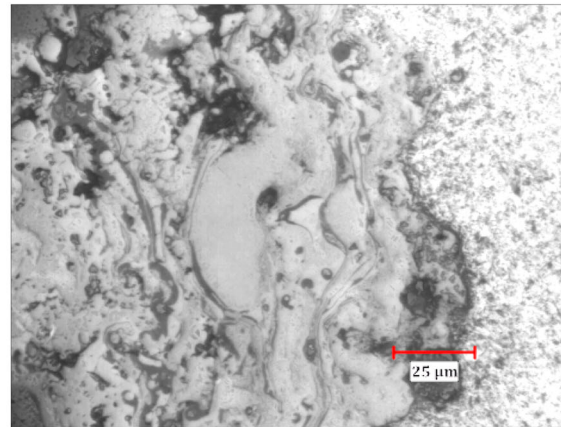


**Fig. 1** a SEM of WC–Co feedstock powder. b EDS of WC–Co feedstock powder

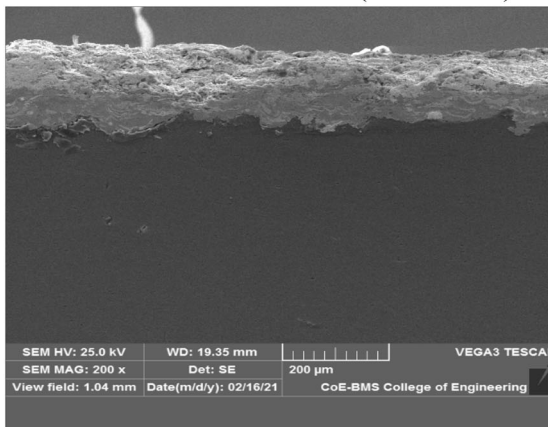




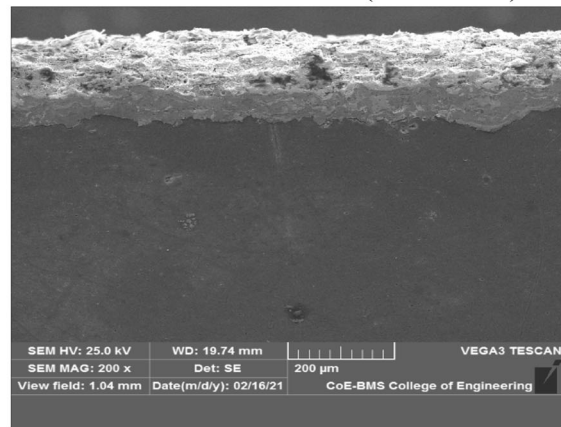
(a) Al6061+WC-10%Co (200 microns)



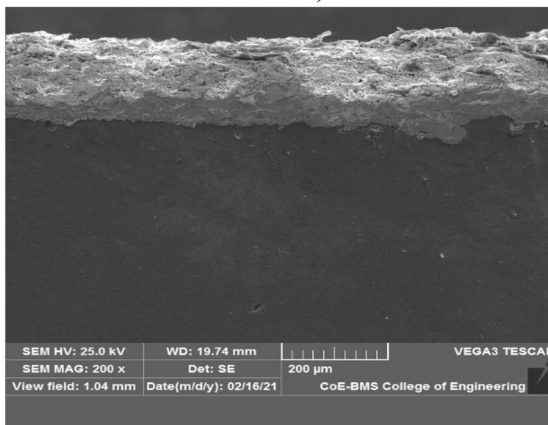
(b) Al6061+WC-20%Co (200 microns)



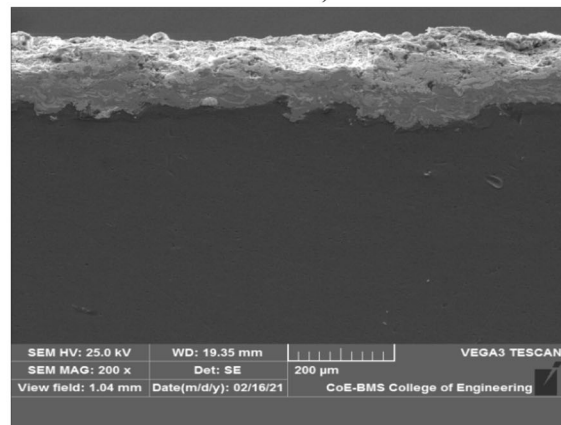
(c) SEM of Al6061+WC-10%Co (100 microns)



(d) SEM of Al6061+WC-10%Co (200 microns)



(e) SEM of Al6061+WC-10%Co (200 microns)



(f) SEM of Al6061+WC-10%Co (200 microns)

**Fig. 2** a Al6061 + WC-10%Co (200 microns). b Al6061 + WC-20%Co (200 microns). c SEM of Al6061 + WC-10%Co (100 microns). d SEM of Al6061 + WC-10%Co (200 microns). e SEM

of Al6061 + WC-10%Co (200 microns). f SEM of Al6061 + WC-10%Co (200 microns)

substrate was observed. The measured thicknesses of WC + 10Co and WC + 20Co coatings are  $100 \pm 15$  microns and  $200 \pm 20$  microns, respectively. Splats of WC-Co particles with spherical shapes have been observed

throughout the microstructure. Cross-sectional images of the coatings show the diameter of ten spherical Ni alloy splats. Figure 3 depicts the SEM of cross section. Large

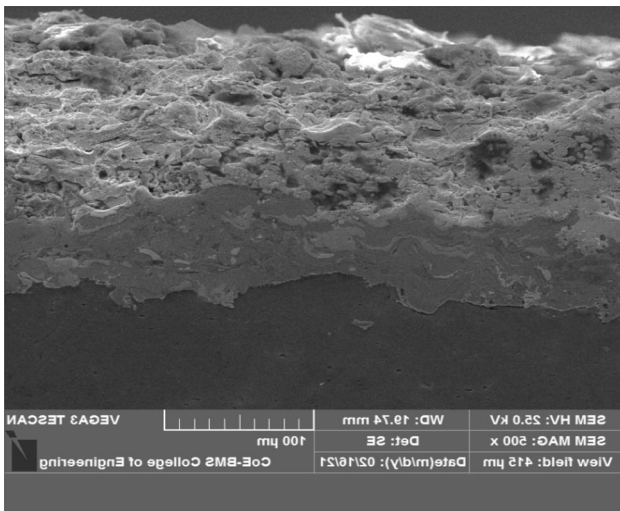


Fig. 3 SEM of Al6061 + WC-20%Co coating

percentages of WC were found in the darker contrast zone, with little Co.

Figure 4 depicts XRD diffractograms of powder feedstock and sprayed coatings. As previously reported [20], the phases found in the WC–Co powder are Co and WC. The as-sprayed coatings contained no  $W_2C$  phase or elemental W during spraying, implying that there was little to no WC decarburization [23].

**Hardness**

The microhardness values obtained from the substrate and WC–Co coatings are shown in Fig. 5. The substrate’s

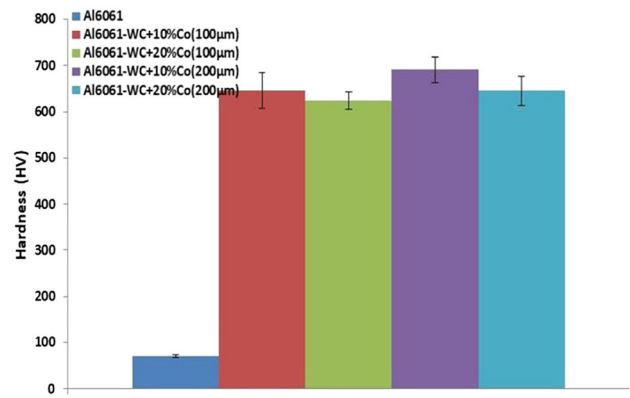


Fig. 5 Comparison of hardness between Al6061 alloy and Al6061 + WC–Co coatings

average hardness value was 71 VHN. The hardness values of the WC-10 percent Co coatings are 645 and 692 VHN for coating thicknesses of 100 microns and 200 microns, respectively. WC-20 percent Co coatings, on the other hand, have hardness values of 624 and 645 VHN for 100 micron and 200 micron coating thicknesses, respectively. The coating’s hardness value is approximately 6 times that of the substrate’s hardness value which can be attributed to the presence of WC in the coatings. It can also be seen that as the cobalt content increases from 10 to 20%, the microhardness of the coating decreases marginally. This could be attributed to the fact that the microhardness of cermet coatings is governed by WC content, while cobalt content contributes less to hardness. Higher hardness and toughness of tungsten carbide increases the microhardness of the coating. Cobalt has a lower hardness than tungsten

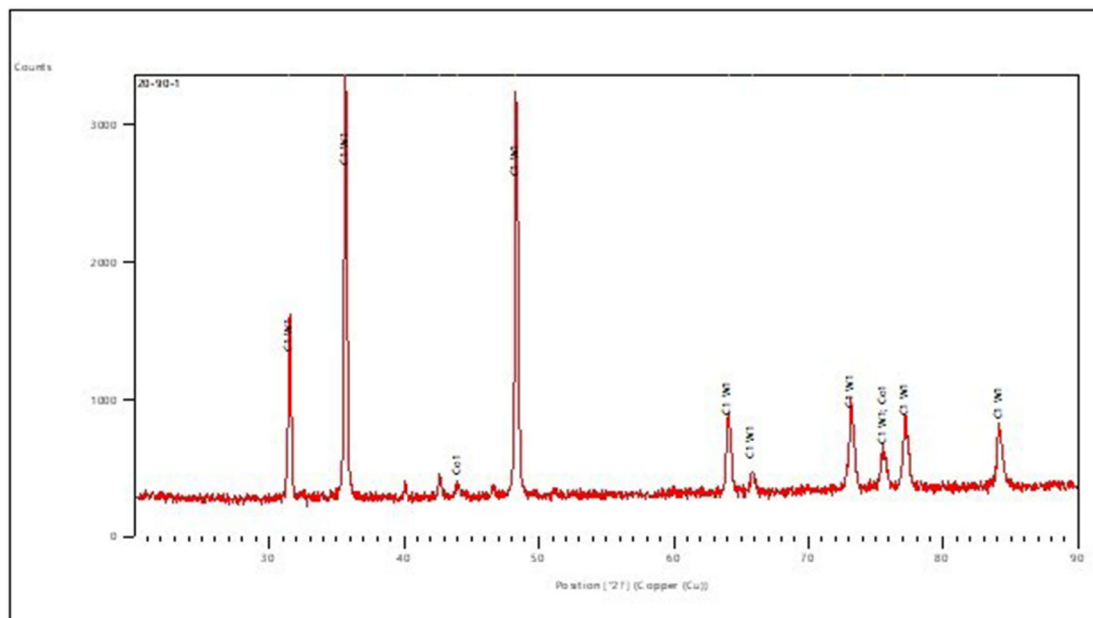
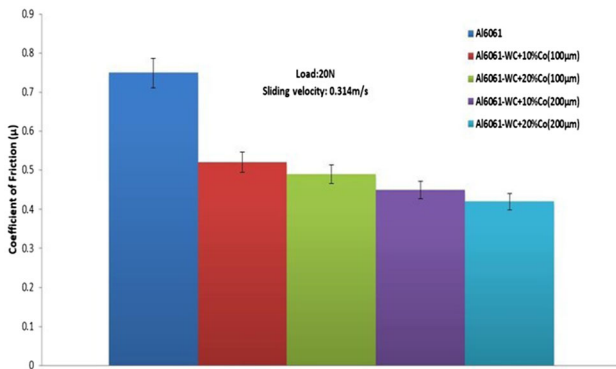


Fig. 4 XRD of SEM of Al6061 + WC-20%Co coating

carbide and increasing the cobalt content resulted in a decrease in hardness. However, as the coating thickness increases, the hardness of the cermet coatings increases marginally in both cases. Another possible reason for higher coating hardness is uniform deposition of the coatings with minimal porosity as a result of optimum process conditions. In terms of coating thickness, WC–Co coatings with a thickness of 200 microns outperformed WC–Co coatings with a thickness of 100 microns. WC-10wt% Co coatings, on the other hand, outperformed WC-20wt% Co coatings in terms of hardness, regardless of coating thickness.

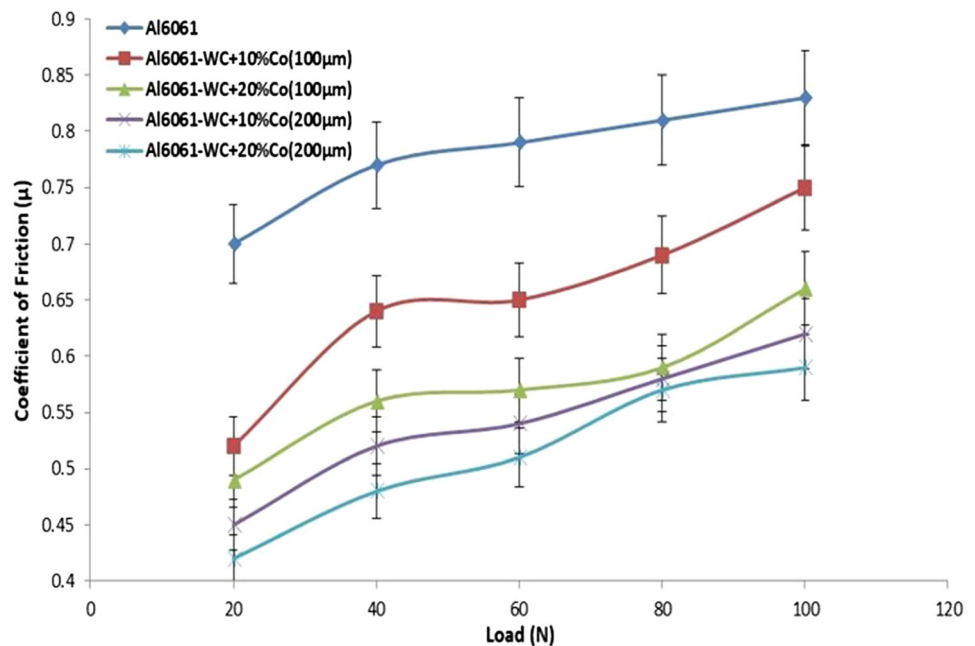
### Coefficient of Friction

Figure 6 depicts the friction coefficient of aluminium alloy and WC–Co coatings with varying thickness and cobalt



**Fig. 6** Comparison of coefficient of friction between Al6061 alloy and WC–Co coatings

**Fig. 7** Effect of load on coefficient friction in alloy and WC–Co coatings



content. At a sliding speed of 0.314 m/s and under an applied load of 20 N, the coefficient of friction was determined. When compared to the uncoated aluminium alloy, the coatings have a significantly lower friction coefficient. It's also worth noting that the coefficient of friction decreases as the coating thickness and cobalt content increase. However, at 200 microns thickness and 20% cobalt content, both coating thicknesses have no effect on friction coefficient. The graph (Fig. 6) shows that for a given set of sliding conditions, WC-10% Co coating with a coating thickness of 100 microns has an average friction coefficient of 0.65, which is 35% lower than the uncoated aluminium alloy. WC-10 % Co coatings with a thickness of 200 microns demonstrated a friction coefficient value of 0.62, which is 0.395 lower than the uncoated alloy. The friction coefficient decreases as the coating thickness increases when compared to alloy; the coefficient of friction improves only slightly when the coating thickness is increased from 100 to 200 microns. On the other hand, it is important to note that as the cobalt content increases from 10 to 20%, the coefficient of friction decreases significantly for both the coating thickness. This could be attributed to the antifriction properties of cobalt in ceramic coatings. Regardless of the sliding or loading conditions, the WC–Co coatings improved the coefficient of friction significantly. WC–Co cermet coatings are known to form a  $\text{CoWO}_4$  and  $\text{WO}_3$  tribo film, which acts as a strong lubricant on the worn surface and reduce the friction coefficient. The oxide  $\text{CoWO}_4$  comprises of  $\text{CoO}$  and  $\text{WO}_3$ , which improves antifriction properties.

Figure 7 depicts the variation of the coefficient of friction with increasing load values for various coating

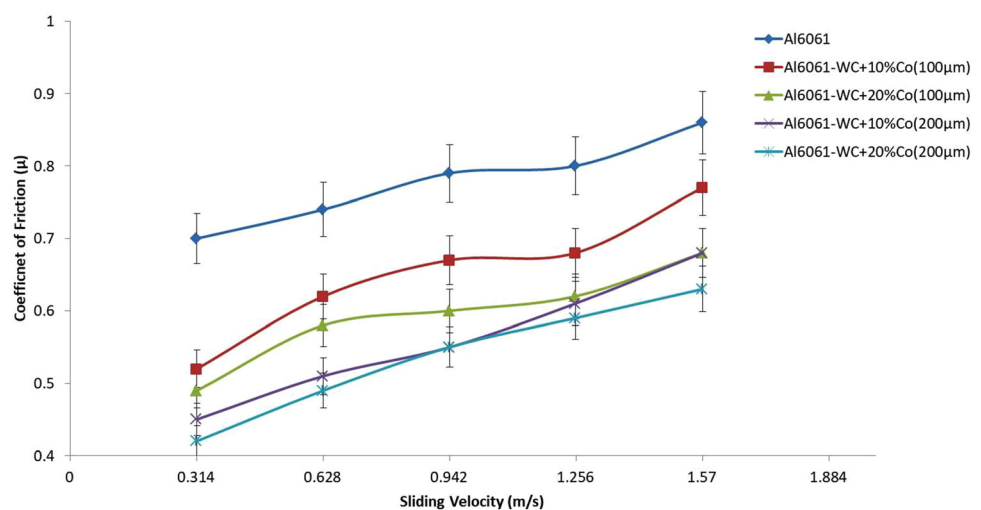
thicknesses and cobalt content. To assess the effect of load on friction coefficient, the load was increased from 20 to 100 N in increments of 20 N while keeping the sliding velocity constant. As the applied load increases, the coefficient of friction of both alloys and coatings increases. When the load was increased from 20 to 100 N, the friction coefficient for alloy increased from 0.23 to 0.45. For WC-20% Co coatings with a thickness of 200 microns, the friction coefficient increased from 0.45 to 0.67 for loads of 20 N and 100 N, respectively. The contact stress generated at the interface between the specimen and in the actual contact regions, the counter disc is comparatively less, resulting in a lower coefficient of friction.

Tribo-chemical reactions on the sample's surface with atmospheric oxygen and moisture result in the formation of a tribo-film. This tribo-film acts as a barrier between the mating surfaces, reducing frictional values at lower loads by separating the actual surfaces, whereas the actual contact area increases with higher loads and higher interface stresses. The coefficient of friction increases as contact stresses exceed the shear strength of the tribo-film, resulting in actual surface contact [10, 15–18]. Formalised paraphrase furthermore, cobalt was added to aid in the achievement of improved coating densification due to its lower melting temperature when compared to tungsten carbide, as well as to improve tribological properties. The friction coefficient is reduced in a complex way as a result of this. As can be seen, the coefficient of friction with load varies dramatically for both the substrate and the WC–Co coating. These variations can be attributed to changes in wear mechanisms at higher and lower loads. The higher toughness of the deposited coatings demonstrates improved plastic deformation rate as well as on the surface of the coating aids the progress of the rapid formation of tribo-layer, resulting in better tribological performance. Coating reduces coefficient of friction by 22% and 21% when

compared to aluminium alloy at load values of 20 N and 100 N, respectively. The increased cobalt content resulted in a beneficial reduction in the coefficient of friction for all loads studied, most likely due to the formation of cobalt oxides, as previously discussed. The effect of increasing coating thickness has also contributed to a reduction in coefficient of friction. When compared to increased cobalt content, an increase in coating thickness has had a significant impact. This could be due to the lower hardness of the coatings with increased cobalt content. However, increased thickness has resulted in higher hardness with dense and uniform coating deposition.

Figure 8 depicts the effect of sliding velocity on the variation of the friction coefficient of aluminium alloy and WC–Co coatings. The sliding velocity was varied from 0.314 to 1.57 m/s under a constant load of 20 N. The graph shows that as the sliding velocity increases, the coefficient of friction for both the substrate and the coatings increases. In comparison to aluminium alloy, WC–Co coatings have an extremely low coefficient of friction at all sliding velocities studied. As the sliding velocity increased from 0.314 to 1.57 m/s, the friction coefficient increased from 0.49 to 0.71 for WC–Co coatings and from 0.46 to 0.56 for aluminium alloy. The increase in coating thickness and cobalt content has resulted in a decrease in friction coefficient. The change in friction coefficient values as sliding velocities increase could be attributed to a shift in oxidation regimes. Interfacial temperature values at lower sliding velocities are typically low because there is enough time for frictional heat transmission due to lower frictional temperature. A mild to moderate oxidation regime will be active at lower sliding velocities. Higher sliding velocity, on the other hand, would result in an insufficient interval for frictional heat transfer, resulting in a higher flash temperature at the interface. As the flash temperature changes, the oxidation regime shifts from moderate to

**Fig. 8** Effect of sliding velocity on coefficient friction in alloy and WC–Co coatings





extreme, resulting in higher frictional values. In comparison to aluminium alloy, WC–Co has shown a reduction of friction coefficients of 24% and 21% with sliding speeds of 1.57 m/s and 0.314 m/s, respectively, for WC-20% Co coatings with 200 microns coating thickness.

## Wear

The wear rate assessments between aluminium alloy and WC–Co coatings of different thickness and cobalt composition are shown in Fig. 9 for a specific set of test circumstances. The wear rate of the WC–Co coating is substantially lower at the same sliding speed and load compared to that of the aluminium alloy. The graph demonstrates a 35% reduction in aluminium alloy wear rate at sliding speeds of 0.314 m/s and a specified load of 20 N. As indicated above, this decrease in wear rate is due to the enhanced hardness and superior tribological characteristics of WC–Co coatings. The increasing thickness of the coating considerably decreases the wear rate for both compositions. Overall, the trend seen with different coating thickness and cobalt content is in line with microhardness. The wear rate was lowest when coated with the maximum hardness, whereas the wear rate was highest when coated with the lowest hardness. The higher wear rate of WC-20% Co compared to WC-10% Co may be due to decreased fracture toughness and hardness of coatings as a result of transitioning from fracture to plastic deformation as a wear mechanism. The coating thickness, hardness, toughness, and composition of the coating usually increase the wear resistance of the coatings together.

The difference in wear rate between aluminium alloy and WC–Co coatings is shown in Fig. 10. At a constant sliding speed of 0.157 m/s, the load exerted ranged from 20 to 100 N. The figures demonstrate that the wear rate of aluminium alloys and WC–Co coatings is increasing as the load increases. However, WC–Co coatings demonstrate a substantially less wear rate for all examined loads compared to

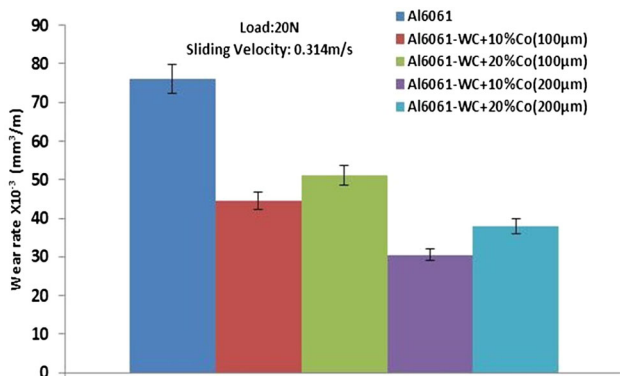


**Fig. 9** Comparison of wear rate between Al6061 alloy and WC–Co coatings

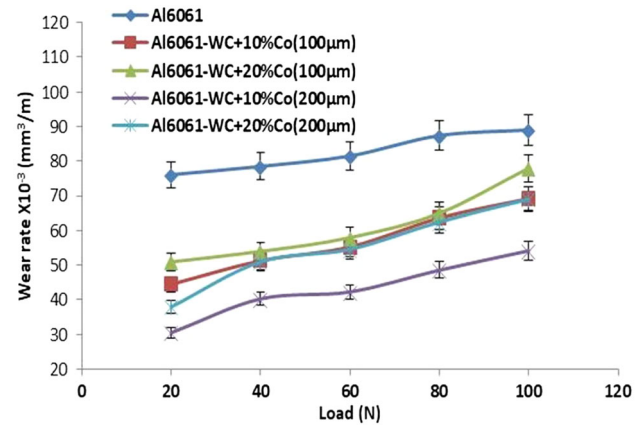


**Fig. 10** Effect of load on wear rate in alloy and WC–Co coatings

aluminium alloys. The wear rate has risen from  $76.1 \times 10^{-3} \text{ mm}^3/\text{m}$  to  $77 \times 10^{-3} \text{ mm}^3/\text{m}$  and from  $54 \times 10^{-3} \text{ mm}^3/\text{m}$  to  $66 \times 10^{-3} \text{ mm}^3/\text{m}$  with the increasing load from 20 to 100 N for aluminium alloy and WC-20% Co coatings (200 µm), respectively. While all filtered coatings showed a decreased wear rate for all loads evaluated, WC-10 % Co, 200 microns thick, had the lowest wear rate followed by WC-20 % Co, 200 microns thick and WC-10 % Co, 100 microns thick. This clearly demonstrates the exceptional wear strength of HVOF sprayed WC–Co coatings for both greater and lower loads with lower cobalt content and higher coating thickness. The WC–Co coating, which offers outstanding antifrictional characteristics with greater oxidation and resistance to wear as well as a higher hardness and substantially higher fracture toughness, can be ascribed to these enhanced wear resistance. The wear rate for WC-20 % Co coating with a thickness of 200 microns was decreased by 43% and 45% at load values of 20 N and 100 N, respectively compared to aluminium alloy.

Figure 11 shows variations in wear rate with sliding speed for WC–Co coating and aluminium alloy. The

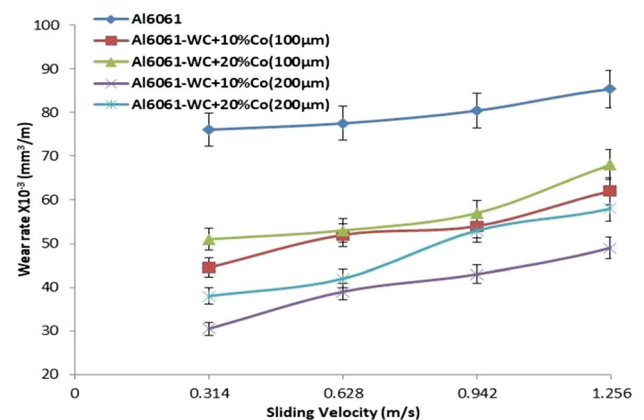


**Fig. 11** Effect of sliding velocity on wear rate in alloy and WC–Co coatings



sliding speed for a given load of 20 N was found to change from 0.314 to 1.57 m/s. The graph indicates that the wear rate for aluminium alloys and WC–Co coatings is increased as the sliding speed rises. All HVOF WC–Co coatings of different layer thickness exhibited a substantial increase in wear at all the investigated sliding speeds compared to aluminium. Although all deposited layers showed reduced wear rates for all sliding speeds evaluated, WC-10 % Co with the thickness of 200 microns demonstrated the lowest wear rate compared to the WC-20 % Co with the thickness of a 200 micron layer, and WC-10 % Co with a thickness of 100 microns. This shows clearly that HVOF spray WC–Co coatings offer incredible resistance to wear at both lower and higher sliding speeds with increased coating thickness and lower cobalt content. Aluminium alloy wear rate rose from  $56 \times 10^{-3} \text{ mm}^3/\text{m}$  to  $65 \times 10^{-3} \text{ mm}^3/\text{m}$  with an increase in sliding velocity from 0.314 to 1.57 m/s to  $67 \times 10^{-3} \text{ mm}^3/\text{m}$  with a thickness of  $67 \times 10 \text{ mm}^3/\text{m}$  for WC-10 % Cobalt. Compared with aluminium alloy, the increased hardness and toughness of the coatings result in a reduced wear rate of the HVOF aluminium layer. As coating's surface hardness improves, its wear and seizure resistance also increases. As already mentioned, the increased toughness of fractures with WC–Co layers contributes to higher wear performance relative to uncoated aluminium alloys. Sliding speeds of 1.57 m/s and 0.314 m/s are 54 and 44% lower respectively than uncoated aluminium alloys.

### SEM Analysis of Worn-out Surfaces

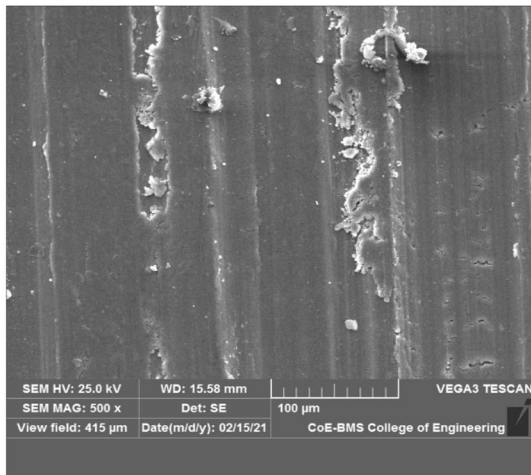
The micrographs of worn-out surfaces of WC–Co coatings and aluminium alloy are presented in Figs. 12 and 13. Micrograms show morphology of depleted WC–Co coated surfaces as well as aluminium alloy evaluated at lower sliding speeds (0.314 m/s) and lower loads (20 N), larger sliding speeds (1.57 m/s) and loads (100 N). Under comparable test circumstances, the morphology of worn-out aluminium and WC–Co coatings, as illustrated in the micrographs, is totally contradicting. Deep and wide grooves go over the aluminium alloy surface (Fig. 12a, b). Meanwhile, extremely fine grooves are observed on the coated surfaces.

For example, the alloy exhibits groove widths of almost 80 microns and 50 microns, respectively, under loading conditions of 100 N and 20 N. The groove width decreased to 50 and 30 microns, respectively, in the case of coatings with the same load values. Similarly, at sliding speeds of 0.314 m/s and 1.57 m/s aluminium alloys have groove widths of around 60 and 100 microns, respectively. For WC–Co coatings, the groove width is 30 and 80 microns at speeds of 0.314 m/s and 1.57 m/s respectively with 20 N

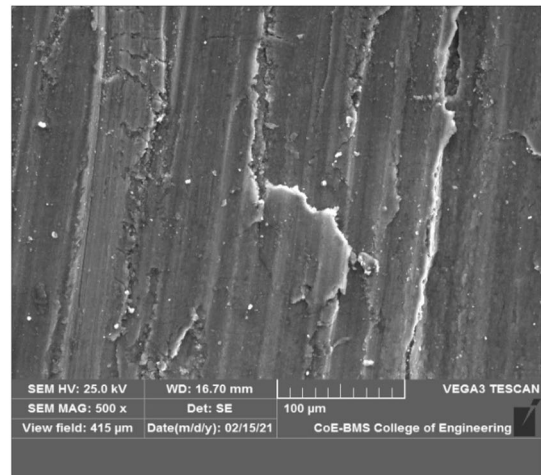
load. This clearly indicates that WC–Co coatings have significantly lower wear rate than bare metals. In determining wear processes of coatings, understanding the coating fracture mechanism is crucial. Plastic deformation cracks and wear debris formations characterise coating surfaces which suggest presence of abrasive and adhesive wear. Some images reveal the existence of worn scrap. It is to be noted that the quantity of wear loss on a worn-out surface often seems to increase as the load increases. More splits in the SEM images can be spotted at greater sliding speeds and loads. The cracks proliferate and induce division and fracture, leading to flaccid development during the sliding process. In addition, coatings show sticky and severe deformations in plastic at greater loads and sliding speeds.

Alloy has broad and deep grooves on worn surfaces with a totally distinct morphology, unlike WC–Co coatings. These studies indicate that the WC–Co coatings exceed wear performance on wear-out surfaces in terms of alloy coatings. Wear debris seems to be oxidised on the worn out surface of WC–Co layers (Fig. 13d, f) due to the interfacial temperature generated during the sliding process. This shifts to a counter-sliding surface and reduces wear and friction. As seen in the damaged surface, these oxidised particles create a protective oxide layer also known as a tribolayer, resulting in enhanced tribological properties, according to several studies [7–10]. Moreover, as demonstrated in Figs. 12 and 13, the aluminium alloy has a strong plastic flow at higher loads and sliding speeds. On the other hand, such morphologies are not seen in WC–Co coatings. It must be noted that the breadth and depth of the slides in uncoated aluminium alloys grow significantly with the increase in load and sliding speed. However, with WC–Co coatings these changes are not evident. Severe plastic distortions, especially in the pictures, were found at greater loading and sliding speeds (Fig. 12). The morphology of uncoated alloys and WC–Co coated surfaces has been shown in micrographs with a greater speed (1.57 m/s), lower load (25 N) and lower sliding speed (0.314 m/s). In determining wear processes of coatings, coating fractures are crucial. Plastic deformation and creation of cracks carry detritus characteristics of worn coating surfaces, involving abrasive and adhesive wear processes. Wear debris is plainly evident in pictures (Fig. 12c–f). It should also be observed that the quantity of wear debris on worn-out surfaces seems to grow as the load increases.

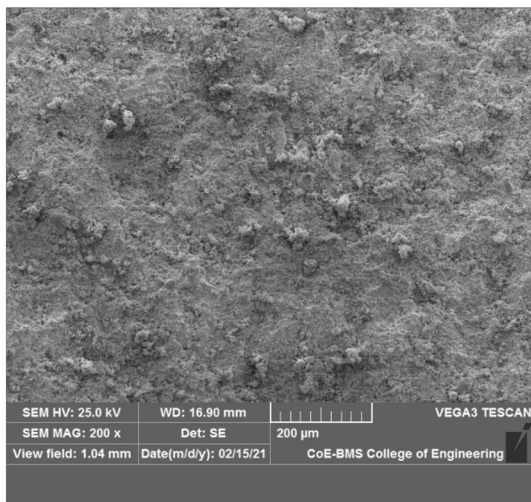
Sliding speeds and increased loads have resulted in a greater number of cracks, as shown in the image (Fig. 13a, b, d, f). The sliding process causes cracks to spread and cause fractures and separation that leads to the development of flakes. Coatings can also have significant plastic deformations and adhesive degradation at greater sliding speeds and loads.



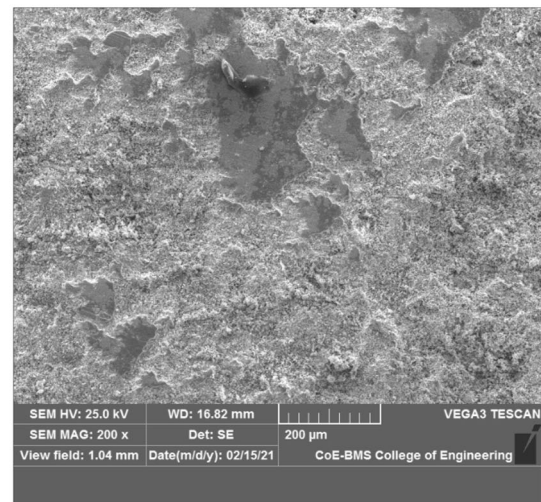
(a) Al6061 Alloy (20N)



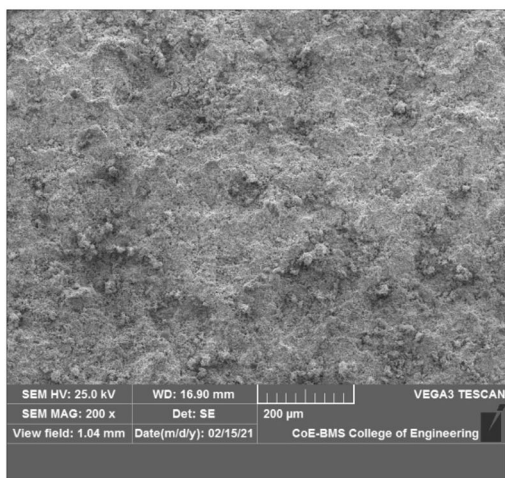
(b) Al6061 Alloy (100N)



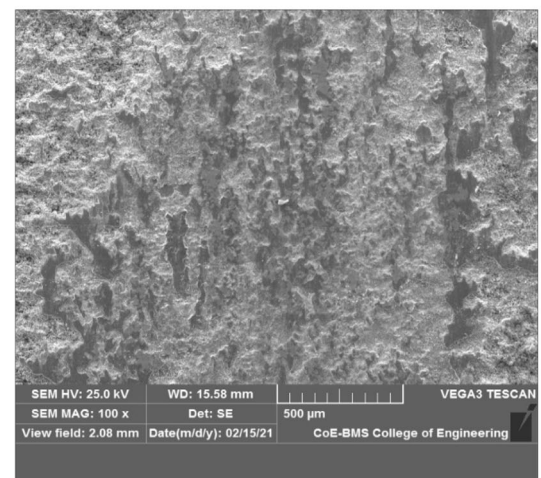
(c) WC-10Co coatings (100 microns) (20N)



(d) WC-10Co coatings (200 microns) (100N)

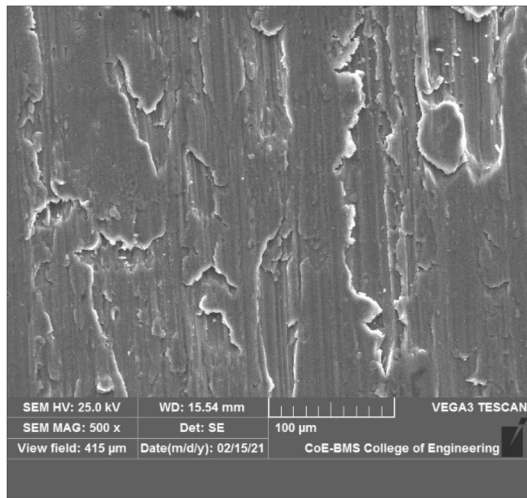


(e) WC-20Co coatings (100 microns) (20N)

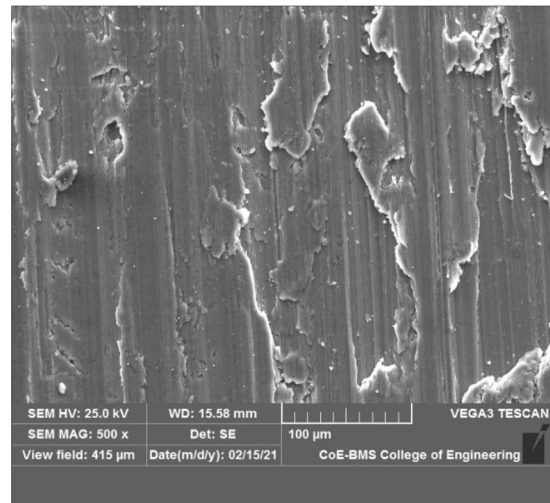


(f) WC-20Co coatings (200 microns) (100N)

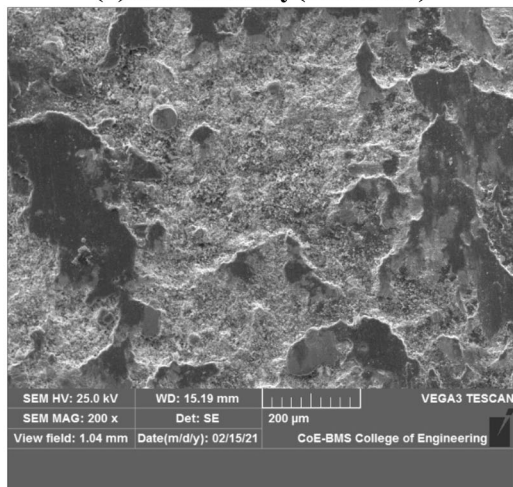
**Fig. 12** SEM of worn out surfaces of Al6061 alloy and WC–Co coatings at different loads



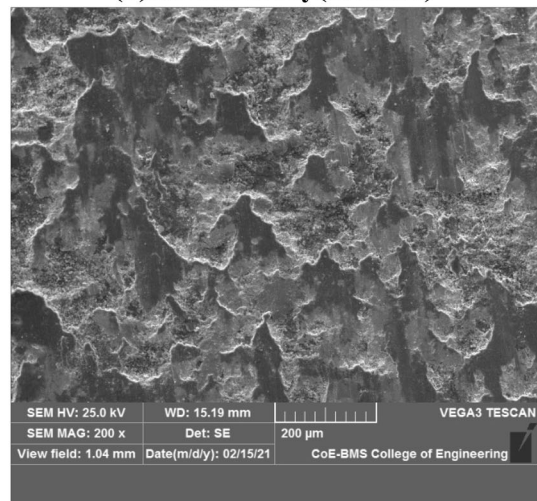
**(a) Al6061 Alloy (0.314 m/s)**



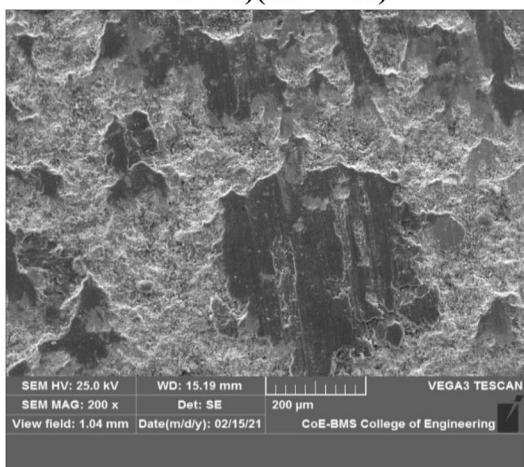
**(b) Al6061 Alloy (1.57 m/s)**



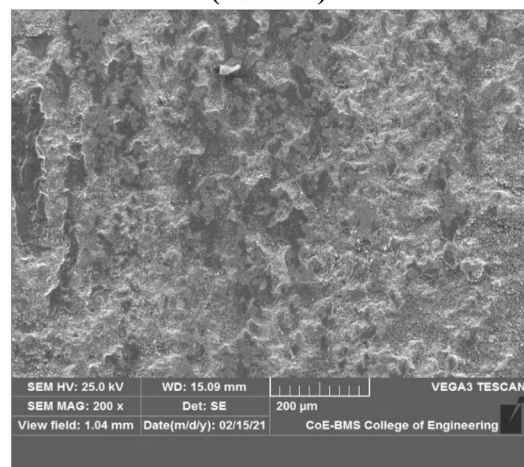
**(c) WC-10Co coatings (100 microns) (0.314 m/s)**



**(d) WC-10Co coatings (200 microns) (1.57 m/s)**



**(e) WC-20Co coatings (100 microns) (0.314 m/s)**



**(f) WC-20Co coatings (200 microns) (1.57 m/s)**

**Fig. 13** SEM of worn out surfaces of Al6061 alloy and WC–Co coatings at different sliding velocities

The wear debris seems to be oxidised on the worn out surface of the aluminium coated alloy (Fig. 13b) because of the interface heat created during the sliding process. They are transferred to a sliding surface which results in a decreased wear rate and friction coefficient. These oxidised particles create a surface layer known as a tribolayer that works as a protective oxide layer and leads to better tribological characteristics. Figure 13a, b demonstrates intensive plastic flow in uncoated aluminium alloys with increasing loads and sliding speeds. However, similar morphologies in WC–Co coatings are not seen. It is important to note that the depth and breadth of the grooves in uncoated aluminium alloys grow as the sliding velocity and load rise. However, these changes are minimal for WC–Co coatings. Severe plastic deformation was found, especially in the pictures at higher loads and sliding speeds (Figs. 12a, f and 13a, f).

Overall, the WC–Co coatings with 200 microns thickness are less damaged for lower and greater loads and sliding speed than the WC–Co surfaces with 100 microns thickness. This confirms the observed trend in friction and wear rates. As the cobalt wt % grows from 10 to 20%, the degree of damage increases both at lower and higher loading rates as well as with increasing sliding speeds. These findings may be seen clearly in the SEM of WC–Co coatings of different compositions. On the worn-out surface, little pores are most likely locations where the material is taken out. Scratches may be observed parallel with the opposite body direction on both coatings. This implies that abrasive wear is one process in this tribological system, which is shown by the presence of grooves on the worn surface created by plugging a harder substance in soft areas. The tracks created against the steel counter body in the uncoated alloy are significantly broader than the wearing scars formed in WC–Co coatings. The pictures of the region at greater magnification, demonstrate an area with worn-out surface properties with fracture processes. The increased surface hardness of WC–Co coatings is probably the cause of the reduced damage. The coated cross-sectional SEM pictures in Fig. 2 demonstrate that porosity exists in these locations, and stresses are more likely to concentrate on areas of porosity in the material, utilising the concepts of linear elastic fracture mechanics, resulting in fractures spreading out from such areas. When hard particles pull away, the abrasion marks are blocking from the coating surfaces with the counter body, as shown in Fig. 8. Due to the friction generated by connection between the counter body and the loaded coating surface, the trapped particles begin to react with oxygen from the atmosphere, forming oxides.

## Confocal Microscopy

The 3D confocal pictures of used aluminium alloys and WC–Co coating are presented in Fig. 14 with 20 N load and a sliding speed of 0.314 m/s. In all the instances investigated, the level of damage in the case of alloys is larger than in the case of WC–Co coatings. The grooves appear to be the largest in the alloy, showing poor resistance to wear. On the other hand, WC–Co coatings feature grooves and pits with significantly smaller widths and heights than aluminium. When compared with WC–Co coatings, aluminium alloy surfaces are considerably too sharp and rough. These data significantly confirm the experimental results that show improved wear resistance of WC–Co-coatings. As illustrated in Fig. 14c–f, WC–Co coatings have less surface damage than alloy substrates. These results demonstrate the enhanced wear characteristics of WC–Co coatings. Although the contour pattern in aluminium is relatively modest, deep grooving has been shown to develop owing to material effect on the surface. Compared to HVOF coatings, the coating surfaces are highly common, as shown by testing and SEM findings.

The optimal wear damage levels for WC–Co coatings were shown to be lower than for aluminium alloy. Damaged alloy surfaces as well as 3D surface morphologies of the WC–Co coatings are shown in Fig. 14a, b. In all circumstances investigated, the damaged surface contours of the aluminium alloy samples showed irregular surface roughness with uneven maxima. It is apparent that the reduced surface damage morphology of coatings suggests higher wear resistance compared to alloy.

Severe wear on the surface of the alloy was detected in Fig. 14a, b, whereas plastic flow and wear scars (Fig. 14c, d) was found in coated specimens. This data confirm the reduced wear rate of the coated substrate surface compared to the bare substrate surface. The loss of material by high shear and plastic flow is clearly shown in Fig. 14a, b. This relation of confocal microscopy is consistent with the results of the experiments.

## Conclusion

The dry sliding friction of HVOF sprayed WC–Co coatings and their wearing efficiencies were studied using disc-pin machine. The sliding wear was analysed at room temperature and the following findings were drawn:

1. Optical and scanning electron micrographs indicate that the WC-10wt % and WC-20wt % coatings are uniformly and densely deposited with little porosity on the aluminium substrate surface.



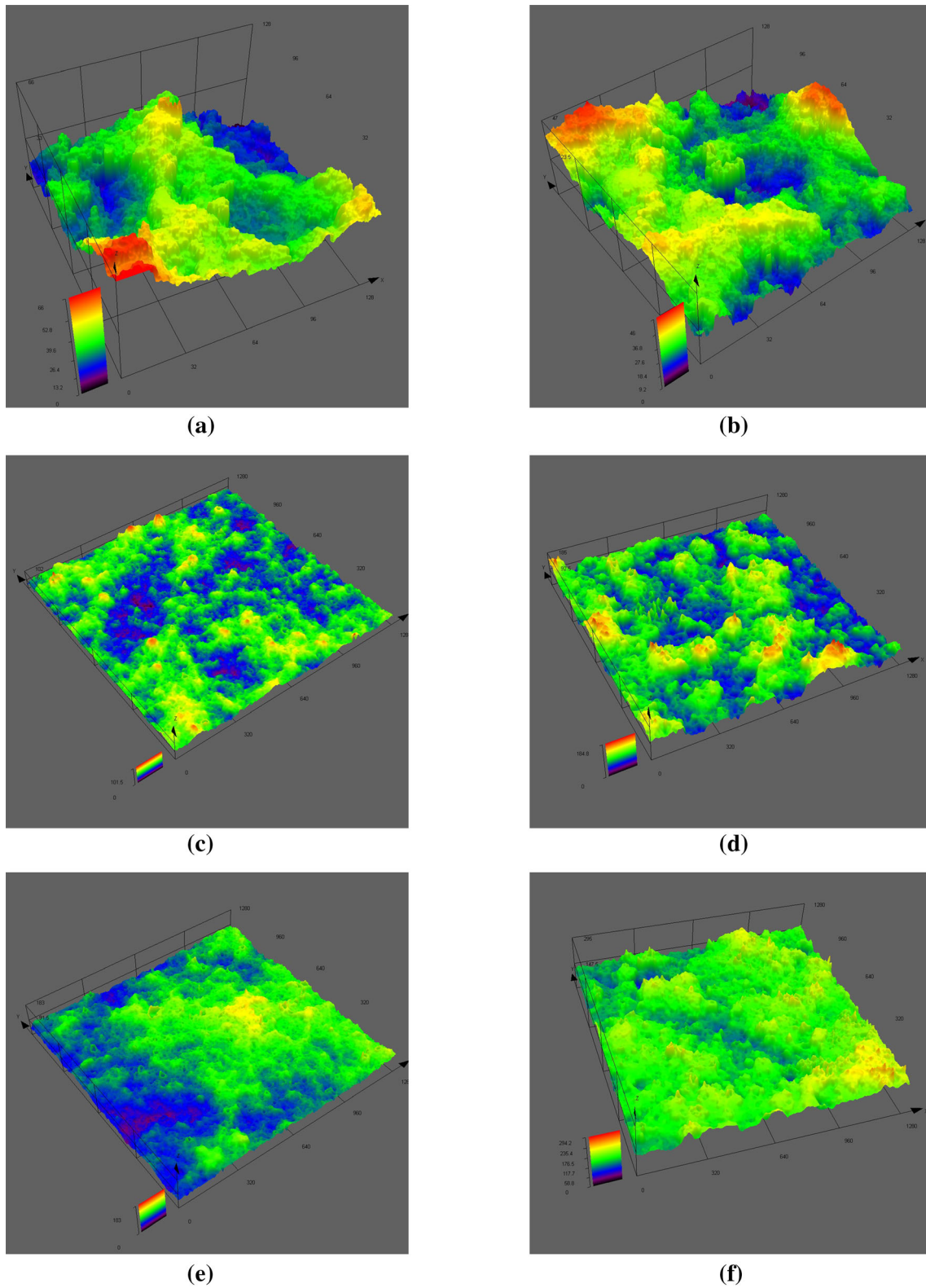


**Fig. 14.** 3D confocal microscopy of worn out surfaces of Al6061 alloy and WC–Co coatings

2. X-ray diffractograms show the existence of both the  $W_2C$  and the WC and cobalt phases.
3. Compared with uncoated alloy, the HVOF sprayed WC–Co coatings showed a better increase in hardness. Hardness of coating reduces as cobalt concentration increases and increases as thickness rises.
4. The developed coatings of the WC–Co have a lower friction coefficient at all sliding speeds and weights than aluminium alloy.
5. The coefficient of friction was lowered by increasing the coating thickness while the wear resistance was enhanced.
6. An increase in cobalt concentration to 20% leads to lesser hardness, lower wear and a greater friction coefficient than WC-10%.
7. SEM and confocal imaging of worn-out surfaces reveal that damage in WC–Co coatings is much minimal than in aluminium alloy.

**Funding** The authors wish to acknowledge their sincere thanks to Vision Group on Science and Technology (VGST) Government of Karnataka, INDIA, for sponsoring this research work (Project No.: KSTePS/VGST/RGS/F/2018-19/GRD-798).

#### Declarations

**Conflict of interest** The Author(s) hereby declare(s) that there is no conflict of interest.

#### References

1. M. Magnani, P.H. Suegama, N. Espallargas, S. Dosta, C.S. Fugivara, J.M. Guilemany, A.V. Benedetti, Influence of HVOF parameters on the corrosion and wear resistance of WC–Co coatings sprayed on AA7050 T7. *Surf. Coat. Technol.* **202**, 4746 (2008)
2. G. Bolelli, L. Lusvardi, M. Barletta, HVOF-sprayed WC–CoCr coatings on Al alloy: effect of the coating thickness on the tribological properties. *Wear* **267**(5–8), 944–953 (2009)
3. A. Karimi, C. Verdon, G. Barbezat, Effect of abrasive particle size on friction and wear behaviour of HVOF sprayed WC-10Co-4Cr coating. *Mater. Res. Express* **5**(6), 066424 (2018)
4. J.A. Picas, E. Rupérez, M. Punset, A. Forn, Influence of HVOF spraying parameters on the corrosion resistance of WC–CoCr coatings in strong acidic environment. *Surf. Coat. Technol.* **225**, 47–57 (2013)
5. Y. Liu, W. Liu, Y. Ma, S. Meng, C. Liu, L. Long, S. Tang, A comparative study on wear and corrosion behaviour of HVOF- and HVOF-sprayed WC–10Co–4Cr coatings. *Surf. Eng.* **33**, 63 (2017)
6. J.K.N. Murthy, B. Venkataraman, Abrasive wear behaviour of WC–CoCr and Cr<sub>3</sub>C<sub>2</sub>–20(NiCr) deposited by HVOF and detonation spray processes. *Surf. Coat. Technol.* **200**(8), 2642–2652 (2006)
7. N. Vashishtha, R.K. Khatirkar, S.G. Sapate, Friction and wear behaviour of plasma sprayed Cr<sub>2</sub>O<sub>3</sub>–TiO<sub>2</sub> coating. *Tribol. Int.* **5**(2), 026410 (2018)
8. Y.Y. Ozbek, N. Canikoglu, M. Ipek, The surface properties of WC–Co–Cr based coatings deposited by high velocity oxygen fuel spraying. *Acta Phys. Pol.* **131**, 186–189 (2017)
9. G. Bolelli et al., Tribology of HVOF- and HVOF-sprayed WC–10Co4Cr hardmetal coatings. *Surf. Coat. Technol.* **265**, 125–144 (2015)
10. G. Bolelli, T. Börner, A. Milanti, L. Lusvardi, J. Laurila, H. Koivuluoto, K. Niemi, P. Vuoristo, Tribological behavior of HVOF- and HVOF-sprayed composite coatings based on Fe-alloy + WC–12% Co. *Surf. Coat. Technol.* **248**, 104–112 (2014)
11. D. Toma, W. Brandl, G. Marginean, Wear and corrosion behaviour of thermally sprayed cermet coatings. *Surf. Coat. Technol.* **138**(2–3), 149–158 (2001)
12. Y.Y. Wang, C.J. Li, A. Ohmori, Examination of factors influencing the bond strength of high velocity oxy-fuel sprayed coatings. *Surf. Coat. Technol.* **200**(9), 2923–2928 (2006)
13. E. Novinski, *Third Global Symposium on HVOF Coatings* (University of Tulsa, San Francisco, 1997)
14. J.-G. Legoux, B. Arsenault, V. Bouyer, C. Moreau, L. Leblanc, Evaluation of four high velocity thermal spray guns using WC-10% Co-4% Cr cermets. *J. Therm. Spray Technol.* **11**, 86–94 (2002)
15. M. Hadad, R. Hitzek, P. Buegler, L. Rohr, S. Siegmann, Wear performance of sandwich structured WC–Co–Cr thermally sprayed coatings using different intermediate layers. *Wear* **263**, 691–699 (2007)
16. Y. Ishinari, S. Kuroda, J. Kawakita, *Surf. Coat. Technol.* **201**, 4717 (2007)
17. J. Pirso, M. Viljus, S. Letunovit, Friction and dry sliding wear behaviour of cermets. *Wear* **260**(7–8), 815–824 (2006)
18. J. Yuan, C. Ma, S. Yang, Z. Yu, H. Li, Improving the wear resistance of HVOF sprayed WC–Co coatings by adding sub-micron-sized WC particles at the splats’ interfaces. *Surf. Coat. Technol.* **285**, 17–23 (2016)
19. T. Terajima, F. Takeuchi, K. Nakata, S. Adachi, K. Nakashima, T. Igarashi, Composite coating containing WC/12Co cermet and Fe-based metallic glass deposited by high-velocity oxygen fuel spraying. *J. Alloy. Compd.* **504**, S288–S291 (2010)
20. I.-D. Utu, I. Hulka, V.-A. Serban, Microstructure and abrasion wear resistance of thermally sprayed cermet coatings. *Mater. Test.* **55**(1), 47–50 (2013)
21. V.A. Şerban, D. Uţu, I. Hulka, C. Opreş, Sliding wear behavior of different HVOF sprayed cermet coatings. *Optoelectron. Adv. Mater.—Rapid Commun.* **6**(7–8), 746–749 (2012)
22. H.V. Özkavak, Ş Şahin, M.F. Saraç, Z. Alkan, Comparison of wear properties of HVOF sprayed WC–Co and WC–CoCr coatings on Al alloys. *Mater. Res. Express* **6**(9), 096554 (2019)
23. J. Pulsford, F. Venturi, S. Kamnis, T. Hussain, Sliding wear behaviour of WC-Co reinforced NiCrFeSiB HVOAF thermal spray coatings against WC–Co and Al<sub>2</sub>O<sub>3</sub> counter bodies. *Surf. Coat. Technol.* **386**, 125468 (2020)

**Publisher’s Note** Springer Nature remains neutral with regard to jurisdictional claims in published maps and institutional affiliations.